conditions. Therefore, a comparison of Figs. 6 and 7 with the measured diffraction strain data of Figs. 1 and 2 (obtained on similar but not identical steels) is possible.

For cold-rolled steels a compressive biaxial stress state results (Dölle & Cohen, 1980; Hauk, Vaessen & Weber, 1985; Maurer *et al.*, 1987) exhibiting approximately equal σ_1 and σ_2 values. Multiplying Fig. 7 by -1, it follows that the $\eta = +1$ graphs indeed strongly resemble the measured curves of Figs. 1 and 2. Differences may be due to deviations from $\eta = +1$, different actual magnitudes of σ_1 and/or σ_2 and small texture differences.

The essence, however, is that macro-stresses σ_1 and σ_2 in conjunction with crystallographic texture qualitatively explain the non-linearities observed. No use has to be made of other stress-tensor elements or the so-called stresses of the second kind (Macherauch *et al.*, 1973).

The authors express their gratitude towards Dr Ir Th. H. de Keijser and Mr N. M. van der Pers for providing X-ray diffraction facilities.

The support of Dr P. van Houtte and Mr M. Mine of the Catholic University Leuven, Belgium, is gratefully acknowledged.

References

BRAKMAN, C. M. (1985*a*). *Cryst. Res. Technol.* **20**, 593-618.
BRAKMAN, C. M. (1985*b*). *J. Appl. Cryst.* **18**, 279-295.
BUNGE, H. J. (1982). *Texture Analysis in Materials Science.* London: Butterworths.
DÖLLE, H. (1979). *J. Appl. Cryst.* **12**, 489-501.
DÖLLE, H. & COHEN, J. B. (1980). *Metall. Trans. A*, **11A**, 831-836.
DÖLLE, H. & HAUK, V. (1977). *Z. Metallkd.* **68**, 719-724.
FANINGER, G. & HAUK, V. (1976). *Härterei-Tech. Mitt.* **31**, 98-108.
HAUK, V. (1955). *Z. Metallkd.* **46**, 33-38.
HAUK, V. (1984). *Adv. X-ray Anal.* **27**, 101-120.
HAUK, V., HERLACH, D. & SESEMANN, H. (1975). *Z. Metallkd.* **66**, 734-737.
HAUK, V. & KOCKELMANN, H. (1977). *Z. Metallkd.* **68**, 719-724.
HAUK, V. & KOCKELMANN, H. (1978). *Z. Metallkd.* **69**, 16-21.
HAUK, V., KRUG, W. H. & VAESSEN, G. (1981). *Z. Metallkd.* **72**, 51-58.
HAUK, V. & MACHERAUCH, E. (1984). *Adv. X-ray Anal.* **27**, 81-99.
HAUK, V. & SESEMANN, H. (1976). *Z. Metallkd.* **67**, 646-650.
HAUK, V. & VAESSEN, G. (1985). *Z. Metallkd.* **76**, 102-107.
HAUK, V., VAESSEN, G. & WEBER, B. (1985). *Härterei-Tech. Mitt.* **40**, 122-128.
HILL, R. (1952). *Proc. Phys. Soc. London Sect. A*, **65**, 349-354.
JAMES, M. R. & COHEN, J. B. (1980). *The Measurement of Residual Stresses by X-ray Diffraction Techniques.* In *Experimental Methods in Materials Science*, Vol. 1, edited by H. HERMAN, pp. 1-62. New York: Academic Press.
MACHERAUCH, E. & MÜLLER, P. (1961). *Z. Angew. Phys.* **13**, 305-312.
MACHERAUCH, E., WOHLFAHRT, H. & WOLFSTIEG, U. (1973). *Härterei-Tech. Mitt.* **28**, 201-211.
MARION, R. H. & COHEN, J. B. (1977). *Adv. X-ray Anal.* **20**, 355-367.
MAURER, G., NEFF, H., SCHOLTES, B. & MACHERAUCH, E. (1987). *Z. Metallkd.* **78**, 1-7.
PENNING, P. & BRAKMAN, C. M. (1988). *Acta Cryst.* **A44**, 157-163.

Acta Cryst. (1988). A**44**, 167-176

Distortion-Induced Scattering due to Vacancies in $NbC_{0.72}$

BY K. OHSHIMA* AND J. HARADA

Department of Applied Physics, Nagoya University, Nagoya 464, *Japan*

M. MORINAGA

Toyohashi University of Technology, School of Production Systems Engineering, Tempaku-cho, Toyohashi-shi, Aichi 440, *Japan*

AND P. GEORGOPOULOS AND J. B. COHEN

MATRIX and Department of Materials Science and Engineering, The Technological Institute, Northwestern University, Evanston, IL 60201, *USA*

(*Received* 23 *July* 1987; *accepted* 7 *October* 1987)

Abstract

The diffuse X-ray (and electron) scattering from $NbC_{0.72}$, previously thought to be due to vacancy octahedra, is shown to be dominated by the scattering due to mean-square atomic displacements with wave vectors near the Brillouin-zone boundary. The atomic displacements are similar to those produced by an optical phonon. On the basis of the sign and amplitude of the displacement parameters a model for the environment around a carbon vacancy is proposed.

* Present address: Institute of Applied Physics, University of Tsukuba, Sakura, Ibaraki 305, Japan.

0108-7673/88/020167-10$03.00

The Nb nearest neighbors to a vacancy move away from it, whereas the C neighbors move toward it, and this appears to be due to an enhancement of the strength of the Nb–C bond arising from the presence of vacancies on the C sublattice. There is evidence that these vacancies tend to be correlated along 211 vectors.

Introduction

Transition-metal carbides are interesting compounds for both fundamental and practical reasons. They have extremely high melting points and hardness, but exhibit a metallic conductivity (Toth, 1971; Storms 1967). The compound NbC_x has a wide single-phase region at high temperatures, ranging from $x = 0{\cdot}70$ to 0·99. It has the NaCl structure with large numbers of carbon vacancies, as has been verified by density measurements (Storms, 1967) and structural analysis (Morinaga, Ohshima, Harada & Otani, 1986). Furthermore, these vacancies strongly affect the physical properties of this carbide. For instance, its superconducting transition temperature varies with composition. Although the precise reason for this relationship is not yet clear (Gigri, Szklarz, Storms, Bowman & Mattias, 1962; Toth, Wang & Yen, 1966; Toth & Zbasnik, 1968; Toth, Ichikawa & Chang, 1968), Bowman (1972) has suggested that vacancy ordering may play a role. The Fermi level shifts with C content, and the density of states changes shape (Klein, Papakonstantopoulos & Boyer, 1980). A vacancy band below the Fermi level, occupied by Nb 4*d* electron states, may be involved in stabilizing the structure (Morinaga, Sato, Aoki, Adachi & Harada, 1983). Also, as NbC_x is extremely unreactive (boiling aqua regia does not attack powdered carbide), it can be employed in corrosion-resistant batteries such as an Na/S cell (Geballe, 1976).

If this material is slowly cooled, long-range ordering of the vacancies occurs (Lewis, Billingham & Bell, 1972). In the disordered (quenched) condition, electron diffraction patterns exhibit strong diffuse scattering which has been thought to be due primarily to local ordering of the vacant sites; a sketch of this scattering is presented in Fig. 1. This intensity surface can be described by the equation (Sauvage & Parthé, 1972, 1974)

$$\cos \pi h + \cos \pi k + \cos \pi l = 0, \qquad (1)$$

where h, k, l are continuous variables in reciprocal space. Similar metal carbides and nitrides give a quite similar diffraction pattern (Billingham, Bell & Lewis, 1972). Sauvage & Parthé (1974) attributed this intensity distribution to the presence of octahedra whose corners are a mixture of carbon atoms and vacancies, and with an Nb atom at the center; the arrangement of the carbon atoms and vacancies determines the modulations of the intensity. De Ridder, Van Tendeloo & Amelinckx (1975, 1976) have extended this approach, and applied it to several materials to interpret their diffuse electron scattering. However, all of this previous work has considered only the position and shape of this scattering, but not the actual intensity. Indeed, there are strong indications that important contributions to the intensity arise from local atomic displacements. The static displacements of first-neighbor Nb atoms around a vacancy [estimated from the Debye-Waller factor (Metzger, Peisl & Kaufman, 1983), channelling experiments and lattice statics (Kaufman & Meyer, 1983)] are large, ≃0·1 Å. (The C-atom shifts are estimated to be much smaller, but have not been well determined.) Several anomalies have also been observed in phonon dispersion curves (Weber, 1973).

There has been one study with neutrons of the actual intensity (Moisy-Maurice, de Novion, Christensen & Just, 1981). However, only one plane in reciprocal space was sampled, and in attempting to separate the effects of local order these authors included only the average displacements, not higher moments. From our results, reported below, we estimate that such terms contributed only 1–2% to their data, so that their separation technique was satisfactory. However, measurements with X-rays (Ohshima, Harada, Morinaga, Georgopoulos & Cohen, 1986) reveal that the features of the diffuse scattering may be too sharp to sample properly with the usual collimation employed in neutron diffraction.

A more complete study of the diffuse scattering due to atomic displacements is presented here, in order to unravel the meaning of this diffuse intensity and to provide information on the carbon-atom displacements and more detail on the Nb shifts. It will be shown that the primary causes of the electron and X-ray scattering are the variances in the displacements, and that there are strong correlations in the Nb movements near a vacancy which are due to electronic effects produced by the vacancies.

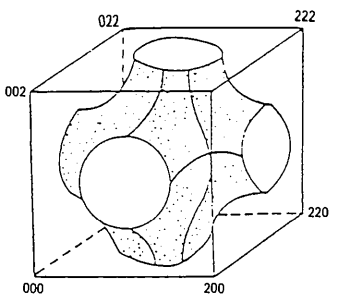

Fig. 1. Shape of diffuse scattering from NbC_x as observed in this study and by Sauvage & Parthé (1972).

Experimental procedures

The crystal

An $NbC_{0.72}$ single crystal was grown by a floating-zone technique in a radio-frequency induction-heated

furnace at 3650 K (Otani, Tanaka & Ishizawa, 1983). It was slowly cooled to 1400 K and then quenched to room temperature. The main impurities were 200–300 p.p.m. oxygen and 160 p.p.m. Ta. An 8 mm diameter disc, 3 mm thick, was cut and polished so that its faces were close to {111} planes. The lattice parameter was measured and found to be 4·436 Å.

Diffraction

The diffuse X-ray scattering in a volume in reciprocal space was obtained with monochromatic radiation (wavelength $\simeq 1{\cdot}5$ Å), in absolute units. The measurements were repeated three times, once with a rotating-anode source at Nagoya University (HIX), once on a bending-magnet line at the Photon Factory in Tsukuba, Japan (PF), and once on the six-pole wiggler line at Cornell University's CHESS facility. After corrections for Compton and parasitic scattering the agreement was quite good; see Ohshima, Harada, Morinaga, Georgopoulos & Cohen (1986) for this comparison, and for further details on the measurements themselves.

Analysis of the diffuse scattering

The deviation from a perfectly periodic array of atoms in a crystal produces diffuse scattering (of X-rays, electrons or neutrons) in addition to the Bragg peaks from the average structure. This 'extra' scattering may be thought of as arising from two effects, one due to the local arrangement of the species (clustering or local order) and the other due to local deviations from periodicity, *i.e.* atomic displacements. When one includes terms up to second order in an expansion of the phase factor $\exp(i\mathbf{k}\,.\,\mathbf{u})$ due to displacements $\mathbf{u}$, the diffuse scattering $I(\mathbf{k})$ is given as the sum of three terms:

$$I_{\rm diff}(\mathbf{k}) = I_{\rm Laue}[I_{\rm SRO}(\mathbf{k}) + I_{\rm SE}(\mathbf{k}) + I_{\rm TDS+H}(\mathbf{k})], \quad (2)$$

where $I_{\rm Laue}$ is the Laue monotonic scattering from a random distribution of the species. The term $I_{\rm SRO}(\mathbf{k})$ is a function of the conditional pair probabilities of finding a B atom at the end of an interactomic vector if there is an A atom at the vector's origin. The second term, $I_{\rm SE}(\mathbf{k})$, is a modulation consisting of terms proportional to $\mathbf{k}$ which provides information about the preferred interatomic distance of any pair. The third term, $I_{\rm TDS+H}(\mathbf{k})$, is the thermal diffuse scattering and a modulation due to the variances in these distances, often called Huang scattering. This effect is proportional to $\mathbf{k}\,.\,\mathbf{k}$.

For this structure, the total diffuse intensity may be written in terms of dimensionless coordinates in reciprocal space, h_i $(i = 1, 3)$, and with $\eta = f_{\rm Nb}/f_{\rm C}$, where the f_i are atomic scattering factors (Hayakawa & Cohen, 1975):

$$\begin{aligned}
I_{\rm diff}(h_i)/I_{\rm Laue} &= I_{\rm SRO}(h_i) \\
&+ h_1 Q_x^{\rm C-C}(h_i) + h_2 Q_y^{\rm C-C}(h_i) + h_3 Q_z^{\rm C-C}(h_i) \\
&+ h_1\eta Q_x^{\rm Nb-C}(h_i) + h_2\eta Q_y^{\rm Nb-C}(h_i) + h_3\eta Q_z^{\rm Nb-C}(h_i) \\
&+ h_1^2\eta^2 R_x^{\rm Nb-Nb}(h_i) + h_1^2\eta R_x^{\rm Nb-C}(h_i) + h_1^2 R_x^{\rm C-C}(h_i) \\
&+ h_2^2\eta^2 R_y^{\rm Nb-Nb}(h_i) + h_2^2\eta R_y^{\rm Nb-C}(h_i) + h_2^2 R_y^{\rm C-C}(h_i) \\
&+ h_3^2\eta^2 R_z^{\rm Nb-Nb}(h_i) + h_3^2\eta R_z^{\rm Nb-C}(h_i) + h_3^2 R_z^{\rm C-C}(h_i) \\
&+ h_1 h_2\eta^2 S_{xy}^{\rm Nb-Nb}(h_i) \\
&+ h_1 h_2\eta S_{xy}^{\rm Nb-C}(h_i) + h_1 h_2 S_{xy}^{\rm C-C}(h_i) \\
&+ h_2 h_3\eta^2 S_{yz}^{\rm Nb-Nb}(h_i) \\
&+ h_2 h_3\eta S_{yz}^{\rm Nb-C}(h_i) + h_2 h_3 S_{yz}^{\rm C-C}(h_i) \\
&+ h_3 h_1\eta^2 S_{zx}^{\rm Nb-Nb}(h_i) \\
&+ h_3 h_1\eta S_{zx}^{\rm Nb-C}(h_i) + h_3 h_1 S_{zx}^{\rm C-C}(h_i). \qquad (3)
\end{aligned}$$

Here,

$$I_{\rm Laue} = N x_{\rm C}^V x_{\rm C}^{\rm C} f_{\rm C}^2, \quad (4)$$

where N is the number of unit cells seen by the incident beam, x_i^j is the sublattice fraction (with subscript indicating the sublattice and superscript the species). With interatomic vector (la, ma, na),

$$\begin{aligned}
I_{\rm SRO}(h_i) = \sum\sum\sum\, &\alpha_{\rm CC}^{\rm C-V}(lmn) \\
&\times \cos 2\pi l h_1 \cos 2\pi m h_2 \cos 2\pi n h_3, \qquad (5)
\end{aligned}$$

and in terms of the conditional pair probability, $P_{\rm CC}^{\rm C-V}$, of finding a vacancy at the end of an interatomic vector on the carbon sublattice, if there is a carbon atom at the vector's origin

$$\alpha_{\rm CC}^{\rm C-V}(lmn) = 1 - P_{\rm CC}^{\rm C-V}(lmn)/x_{\rm C}^V. \quad (6)$$

The short-range-order parameter α has values only for $(l+m+n) = 2p/2$ (with p an integer).

Also, the Q terms involve the fractional displacements X, Y, Z from vectors of the average lattice:

$$\begin{aligned}
Q_x^{\rm Nb-C}(h_i) = \sum\sum\sum\, &\gamma_x^{\rm Nb-C}(lmn) \sin 2\pi l h_1 \\
&\times \cos 2\pi m h_2 \cos 2\pi n h_3 \qquad (7a)
\end{aligned}$$

$$\gamma_x^{\rm Nb-C}(lmn) = 4\pi/x_{\rm C}^V \langle X_{\rm NbC}^{\rm Nb-C}(lmn)\rangle \qquad (7b)$$

$$\begin{aligned}
Q_x^{\rm C-C}(h_i) = \sum\sum\sum\, &\gamma_x^{\rm C-C}(lmn) \sin 2\pi l h_1 \\
&\times \cos 2\pi m h_2 \cos 2\pi n h_3 \qquad (7c)
\end{aligned}$$

$$\begin{aligned}
\gamma_x^{\rm C-C}(lmn) = 2\pi[&x_{\rm C}^{\rm C}/x_{\rm C}^V + \alpha_{\rm CC}^{\rm C-V}(lmn)] \\
&\times \langle X_{\rm CC}^{\rm C-C}(lmn)\rangle, \qquad (7d)
\end{aligned}$$

whereas the R and S terms involve variances in the displacements:

$$\begin{aligned}
R_x^{\rm Nb-Nb}(h_i) = \sum\sum\sum\, &\delta_x^{\rm Nb-Nb}(lmn) \cos 2\pi l h_1 \\
&\times \cos 2\pi m h_2 \cos 2\pi n h_3 \qquad (8a)
\end{aligned}$$

$$\delta_x^{\rm Nb-Nb}(lmn) = 4\pi^2/x_{\rm C}^{\rm C} x_{\rm C}^V \langle X_{\rm Nb}^{\rm Nb}(000) X_{\rm Nb}^{\rm Nb}(lmn)\rangle. \qquad (8b)$$

For $R_x^{C-C}(h_i)$,

$$\delta_x^{C-C}(lmn) = 4\pi^2[x_C^C/x_C^V + \alpha_{CC}^{C-V}(lmn)] \times \langle X_C^C(000) X_C^C(lmn)\rangle. \quad (8c)$$

Both (8*b*) and (8*c*) differ from zero only for $(l+m+n)=2p/2$.

For $R_x^{Nb-C}(lmn)$,

$$\delta_x^{Nb-C}(lmn) = 8\pi^2/x_C^V\langle X_{Nb}^{Nb}(000) X_C^C(lmn)\rangle, \quad (8d)$$

which has a value only for $(l+m+n)=(2p+1)/2$. Finally,

$$S_x^{Nb-Nb}(h_i) = \sum\sum\sum \varepsilon_{xy}^{Nb-Nb}(lmn) \sin 2\pi l h_1 \times \sin 2\pi m h_2 \cos 2\pi n h_3 \quad (9a)$$

where

$$\varepsilon_{xy}^{Nb-Nb}(lmn) = 8\pi^2/x_C^C x_C^V\langle X_{Nb}^{Nb}(000) Y_{Nb}^{Nb}(lmn)\rangle, \quad (9b)$$

and for $S_{xy}^{C-C}(h_i)$,

$$\varepsilon_{xy}^{C-C}(lmn) = 8\pi^2[x_C^C/x_C^V + \alpha_{CC}^{C-V}(lmn)] \times \langle X_C^C(000) Y_C^C(lmn)\rangle. \quad (9c)$$

Both (9*b*) and (9*c*) exist only for $(l+m+n)=2p/2$.

Similarly, for $S_{xy}^{Nb-C}(lmn)$,

$$\varepsilon_{xy}^{Nb-C}(lmn) = 16\pi^2/x_C^V\langle X_{Nb}^{Nb}(000) Y_C^C(lmn)\rangle, \quad (10)$$

which differs from zero only for $(l+m+n)=(2p+1)/2$.

The restrictions on the various coefficients result from the fact that I_{SRO} has f.c.c. symmetry (involving only the carbon sublattice), whereas the Q, R and S terms have simple cubic symmetry and involve terms between sublattices, that is, their unit cell is that for the smaller simple cube in the NaCl cell that arises when the identity of the species is ignored. Equation (3) results from the assumption that the Nb atoms fill one sublattice and that the C atoms and vacancies are on the other sublattice.

Data analysis

Each term in (3) (I_{SRO}, Q, R, S) is a Fourier series, so that if the total intensity can be separated into these 25 component series, inversion will provide the α's and displacements. There are basically two ways to achieve this separation and we attempted both.

(1) The intensity can be sampled at a point in the minimum volume in reciprocal space for I_{SRO} obtained from the symmetry of this term, and at a number of other points related by the symmetries of the components. The separation is then accomplished by least squares (Georgopoulos & Cohen, 1977; Wu, Matsubara & Cohen, 1983), a volume in reciprocal space is filled for each component with the aid of its symmetry and the data in the minimum volume, and this component is then inverted. We actually employed the minimum volume for R and S, which is twice the minimum volume for Q and I_{SRO}. This volume was sampled at intervals h of 0·1. For each such point typically 50 other points were measured for a total of 9000–12 000 points at each of the three radiation sources, which were combined for analysis. (The individual data sets were also analyzed, but only the results of the combination are discussed here.) Although we attempted a complete solution of (3), as has been done for binary alloys (Cohen, 1986), this was not possible; the I_{SRO} term is less than 1% of the total and while the separated values had the shape in reciprocal space anticipated from previous studies, the integrated total exceeded the required value of unity [equation (2*c*) for $lmn=000$]. In (1), and for X-rays or electrons, the terms in R and S dominate (the terms in Q contribute only 10% of the total) and, furthermore, because η is only ~7% of η^2, all the terms involving the carbon atom make a small contribution. Stable solutions for the Q's, R's and S's were found only when I_{SRO} and the C–C and Nb–C terms in R and S were ignored, which reduced (3) to nine terms. Even with this simplification the separated intensity components did not have the correct symmetries, in particular the Q terms. This can lead to non-zero values for the displacements for interatomic vectors when the value should be zero, as mentioned in the *Introduction*. Even the addition of third-order terms did not improve the situation, and therefore this method of analysis was discontinued.

(2) Each component series in (3) can be expanded and the terms limited to a finite number (Williams, 1972). Solutions excluding I_{SRO}, but including 83–113 of all the remaining terms gave reliability indices of 10–12%. This analysis was performed with each of the three experiments separately.

Results

The Fourier coefficients for the least-squares solution are shown in Fig. 2 for the data taken at CHESS and for various numbers of terms. In Fig. 3 the results are given for 83 terms for various ranges of data. These two figures indicate that the solutions are stable. Solutions are given in Fig. 4 for the three sets of data. The agreement is good in all cases, and a comparison of the intensity simulation of one set and the measured intensities is presented in Fig. 5; this figure demonstrates the satisfactory nature of the solutions and also shows that most of the X-ray scattering is due to the terms (R and S) quadratic in the displacements. This must also be the case for the reported electron scattering.

Much of the diffuse scattering is concentrated near the Brillouin-zone boundary (near the K point). The contribution due to thermal effects is therefore small and optical phonon-like modes must be 'frozen in'

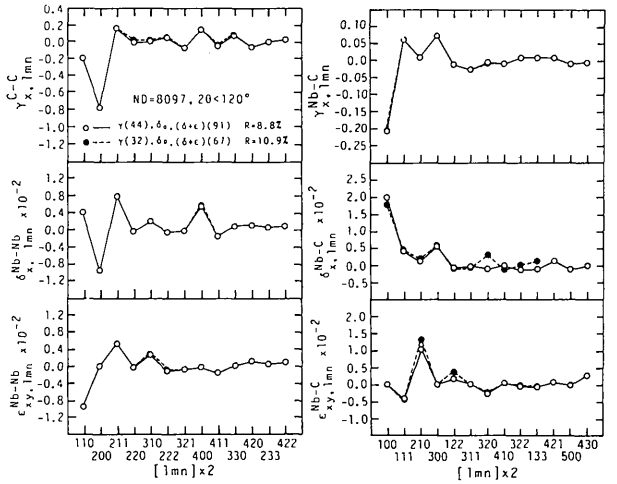

Fig. 2. The Fourier coefficients of the terms in equation (3), for the data taken at CHESS, and for various numbers (shown in parentheses) of terms in the least-squares solution of this equation. ND is the number of data points.

(condensed). The displacements are summarized in Table 1. The elastic constants (Weber, 1973) are quite high (as expected, since the melting point exceeds 3600 K). With these constants, first-, and second- and third-order thermal diffuse scattering were calculated. Their total was only of the order of 0·5% of the observed intensity.

Among the coefficients determined in this analysis, $\delta_x^{\mathrm{Nb-Nb}}(000)$ has a special physical meaning. It is related to the mean-square x component of the static and dynamic displacement of an Nb atom from the average lattice.

$$\delta_x^{\mathrm{Nb-Nb}}(000) = 4\pi^2 / x_C^C x_C^V \langle [X_{\mathrm{Nb}}^{\mathrm{Nb}}(000)]^2 \rangle \quad (11)$$

where X is the displacement as a fraction of the lattice parameter. The Debye-Waller factor can be calculated from this value as $8\pi^2\langle(X^{\mathrm{Nb}})^2\rangle a^2$. With the values in Table 1, the result is 0·373 Å^2, in good agreement with the value of 0·32 (6) Å^2 recently determined from an analysis of integrated intensities of Bragg peaks (Morinaga, Ohshima, Harada & Otani, 1986). This is an additional confirmation of the success of the analysis.

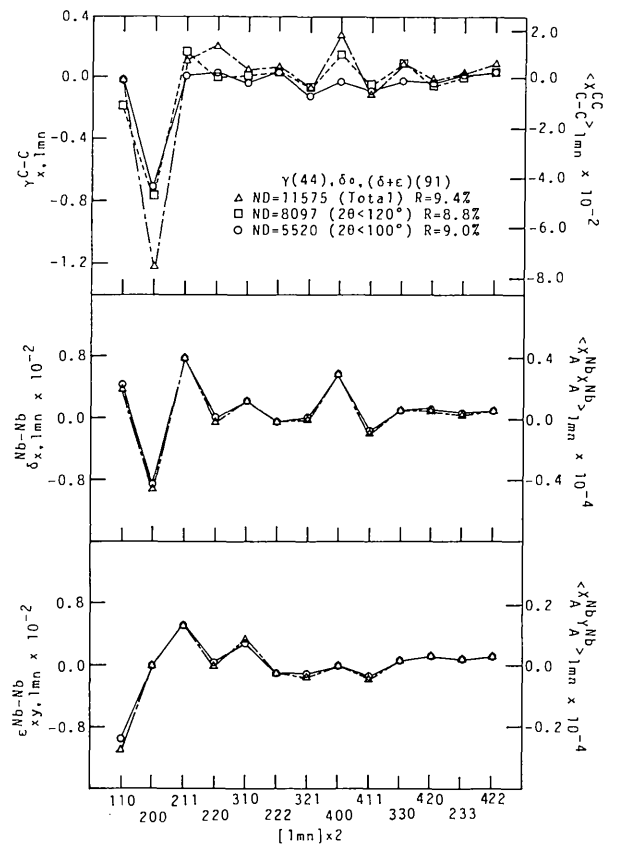

Fig. 3. Fourier coefficients in equation (3) for various ranges of the data in reciprocal space, as indicated.

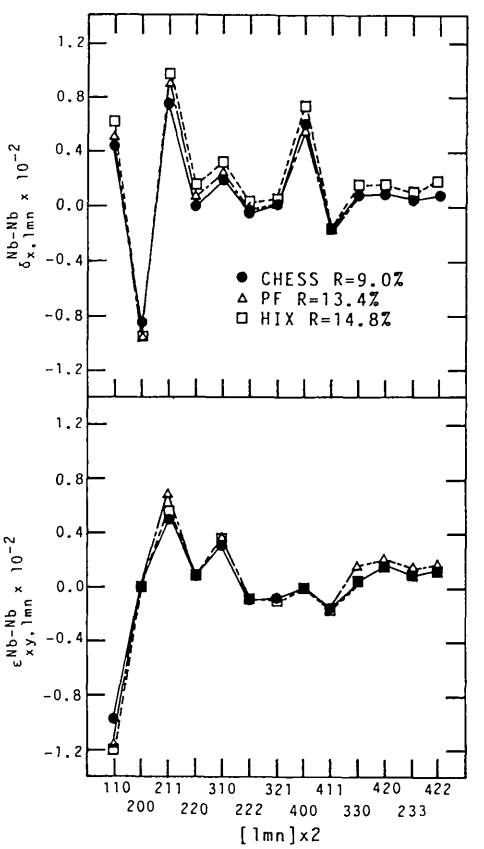

Fig. 4. Comparison of the Fourier coefficients for the three sets of data.

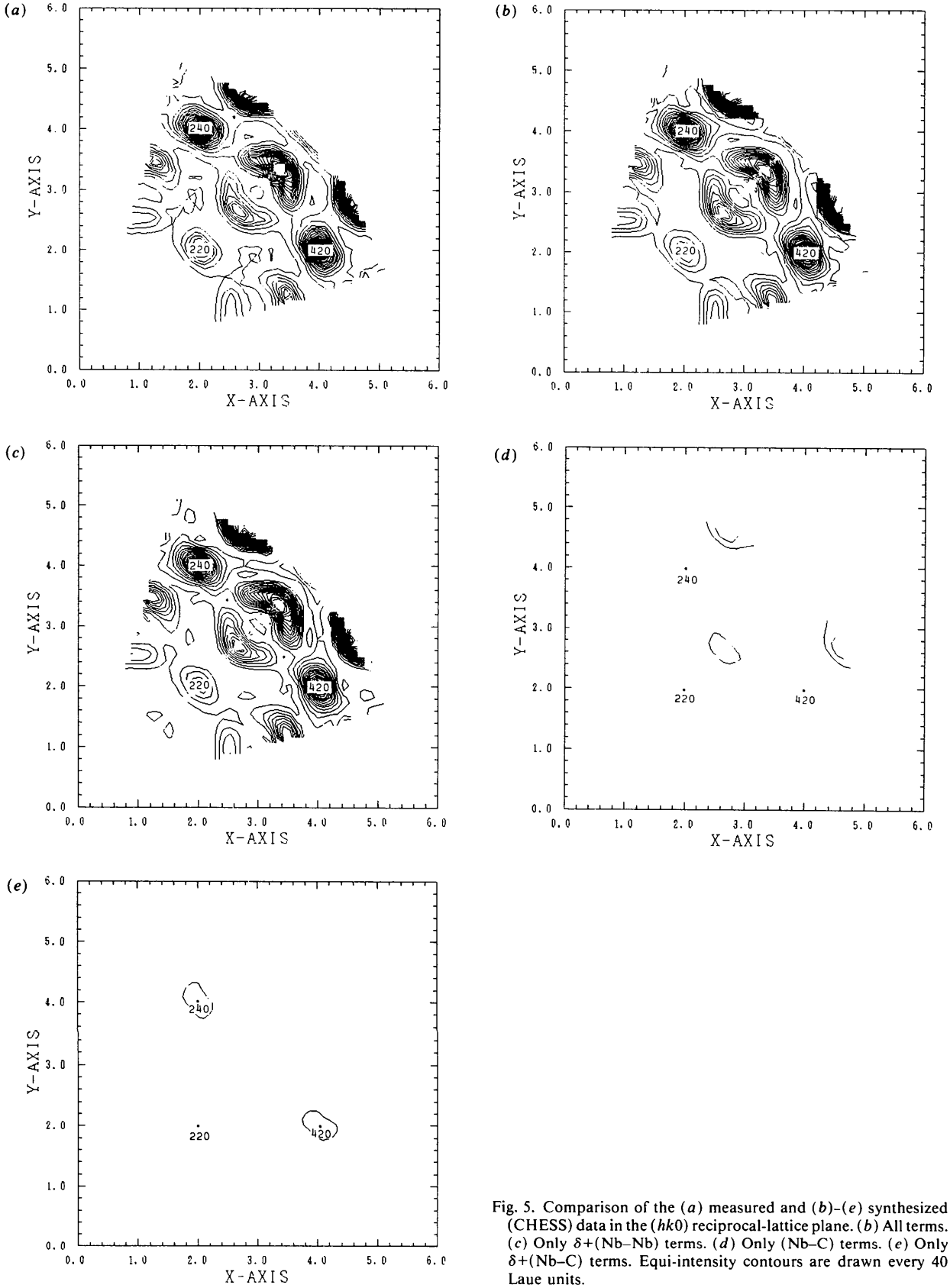

Fig. 5. Comparison of the (*a*) measured and (*b*)-(*e*) synthesized (CHESS) data in the (*hk*0) reciprocal-lattice plane. (*b*) All terms. (*c*) Only δ+(Nb–Nb) terms. (*d*) Only (Nb–C) terms. (*e*) Only δ+(Nb–C) terms. Equi-intensity contours are drawn every 40 Laue units.

Table 1. *List of displacement parameters for* $NbC_{0.72}$

$2x[lmn]$	$\langle X^{CC}_{C-C}\rangle$	$\langle Y^{CC}_{C-C}\rangle$	$\langle Z^{CC}_{C-C}\rangle$	$\langle X^{Nb}_A X^{Nb}_A\rangle$	$\langle Y^{Nb}_A Y^{Nb}_A\rangle$	$\langle Z^{Nb}_A Z^{Nb}_A\rangle$	$\langle X^{Nb}_A Y^{Nb}_A\rangle$	$\langle Y^{Nb}_A Z^{Nb}_A\rangle$	$\langle Z^{Nb}_A X^{Nb}_A\rangle$
Type 1	($\times10^{-2}$)	($\times10^{-2}$)	($\times10^{-2}$)	($\times10^{-4}$)	($\times10^{-4}$)	($\times10^{-4}$)	($\times10^{-4}$)	($\times10^{-4}$)	($\times10^{-4}$)
000	0	0	0	2·43*	2·43	2·43	0	0	0
110	−1·16	−1·16	0	0·21	0·21	−0·28	−0·25	0	0
200	−4·75	0	0	−0·48	0·18	0·18	0	0	0
211	1·02	−0·23	−0·23	0·40	0·09	0·09	0·13	0·00	0·13
220	−0·04	−0·04	0	−0·02	−0·02	0·10	−0·01	0	0
310	0·08	0·03	0	0·10	0·00	0·08	0·07	0	0
222	0·31	0·31	0·31	−0·03	−0·03	−0·03	−0·03	−0·03	−0·03
321	−0·40	−0·46	0·11	−0·01	−0·02	−0·01	−0·02	−0·01	−0·01
400	0·98	0	0	0·28	−0·06	−0·06	0	0	0
411	−0·28	0·12	0·12	−0·08	0·01	0·01	−0·04	0·02	−0·04
330	0·53	0·53	0	0·05	0·05	−0·01	0·01	0	0
420	−0·37	0·17	0	0·06	0·06	−0·00	0·03	0	0
233	0·02	0·24	0·24	0·03	0·03	0·03	0·02	0·02	0·02
422	0·19	0·04	0·04	0·05	0·01	0·01	0·02	0·00	0·02
$2x[lmn]$	$\langle X^{NbC}_{A-C}\rangle$	$\langle Y^{NbC}_{A-C}\rangle$	$\langle Z^{NbC}_{A-C}\rangle$	$\langle X^{Nb}_A X^{C}_C\rangle$	$\langle Y^{Nb}_A Y^{C}_C\rangle$	$\langle Z^{Nb}_A Z^{C}_C\rangle$	$\langle X^{Nb}_A Y^{C}_C\rangle$	$\langle Y^{Nb}_A Z^{C}_C\rangle$	$\langle Z^{Nb}_A Y^{C}_C\rangle$
Type 2	($\times10^{-2}$)	($\times10^{-2}$)	($\times10^{-2}$)	($\times10^{-4}$)	($\times10^{-4}$)	($\times10^{-4}$)	($\times10^{-4}$)	($\times10^{-4}$)	($\times10^{-4}$)
100	−0·46	0	0	0·71	0·20	0·20	0	0	0
111	0·14	0·14	0·14	0·14	0·14	0·14	−0·08	−0·08	−0·08
210	0·02	0·03	0	0·05	0·03	−0·03	0·18	0	0
300	0·17	0	0	0·20	0·07	0·07	0	0	0
122	−0·03	−0·02	−0·02	−0·03	0·07	0·07	0·03	0·02	0·03
311	−0·06	−0·04	−0·04	−0·02	−0·03	−0·03	0·00	0·07	0·00
320	−0·01	0·00	0	−0·04	−0·04	0·10	−0·05	0	0
410	−0·24	0·01	0	−0·00	0·01	−0·04	0·01	0	0
322	0·02	0·01	0·01	−0·05	−0·04	−0·04	−0·01	−0·04	−0·01
133	0·02	0·01	0·01	−0·05	0·01	0·01	−0·01	0·06	−0·01
421	0·02	0·00	0·01	0·05	−0·06	−0·02	0·01	−0·00	0·01
500	−0·02	0	0	−0·04	−0·02	−0·02	0	0	0
430	−0·01	−0·01	0	−0·01	−0·02	−0·02	0·05	0	0

* When $[lmn]$ is [000], $\langle X^{Nb}X^{Nb}\rangle$ becomes $\langle (X^{Nb})^2\rangle$. As the temperature, B_{Nb} is expressed by $8\pi^2\langle (X^{Nb})^2\rangle$, it was estimated to be about 0·37 Å^2. This value is comparable with the B_{Nb} value of 0·32 Å^2 determined by the measurements of integrated X-ray intensities of Bragg reflections.

Discussion

In the present analysis, the following quantities are large:

$$\gamma_x^{Nb-C}(100)<0 \qquad \gamma_x^{C-C}(200)<0$$
$$\delta_x^{Nb-C}(100)>0 \quad \delta_x^{Nb-Nb}(200)<0 \quad \delta_x^{Nb-Nb}(211)>0$$
$$\varepsilon_{xy}^{Nb-C}(210)>0 \quad \varepsilon_{xy}^{Nb-Nb}(110)<0 \quad \varepsilon_{xy}^{Nb-Nb}(211)>0. \tag{12}$$

By trial and error, it was found that the displacements around a C vacancy could satisfy these inequalities, as is illustrated in Fig. 6(*a*). The opposite displacement mode is shown in Fig. 6(*b*), and clearly does not satisfy the first two relationships. No other model could be conceived. Thus, it appears that the first nearest-neighbor niobium atoms move away from a central carbon-atom vacancy, but the second-neighbor carbon atoms move towards this vacancy. Kaufman & Meyer (1983) have recently proposed a model for the local atomic displacements around a single vacancy (based on their ion-channelling and neutron diffraction experiments) that is in agreement with this study. The displacement of the first niobium neighbors along [100] can be estimated from the relation

$$\langle X^{Nb}_{Nb}(000)X^{Nb}_{Nb}(200)\rangle = -x_C^V(1-x_C^V)\langle (X^{Nb})^2\rangle. \tag{13}$$

With the results in Table 1 for the left-hand side of this equation, the displacement is 0·07 Å compared with the value of 0·09 Å for $NbC_{0.82}$ reported by Kaufman & Meyer (1983).

Although the principal parameters in Table 1 can be interpreted with the displacement mode illustrated in Fig. 6(*a*), the magnitude of the displacements seems to be modulated by the local vacancy arrangements. Note that the coefficients $\delta_x^{Nb-Nb}(211)$ and $\delta_x^{Nb-Nb}(400)$ (which correspond to relatively long interatomic vectors) are large and positive. This can be attributed to vacancy–vacancy correlations along 211 vectors, because a vacancy causes large Nb displacements, as seen in Fig. 6(*a*). Intensity simulations [*via* (3)] on the (*hk*0) reciprocal-lattice plane, shown in Figs. 7(*a*)–(*c*), are helpful in establishing the importance of each coefficient. Simulations with coefficients up to 200 vectors (Fig. 7*b*) fail to describe the basic features of the observed diffuse scattering (Fig. 7*a*), whereas the inclusion of 211 coefficients (Fig. 7*c*) results in dramatic improvement. Furthermore, the diffuse scattering is concentrated near the superlattice reflections of Nb_6C_5, which is isomorphous with V_6C_5 (Venables & Lye, 1969). This structure can be described in terms of the stacking of (111) planes. As in the work of Iida (1955), a possible atomic arrangement was constructed and is illustrated in Fig. 8; the vacancy-to-vacancy direction is $\frac{1}{2}\langle 211\rangle$

and corresponds to the third-neighbor shell around a C vacancy. Sauvage, Parthé & Yelon (1974) have reported that the short-range-order parameter $\alpha^{C-V}(200)$ is large and negative, suggesting that a vacancy tends to have C atoms as second neighbors (at ⟨100⟩ positions), similar to VO and TiO (Morinaga & Cohen, 1979; Terauchi & Cohen, 1979). This is actually built into the arrangement shown in Fig. 8. At least two of the observed inequalities (12) are satisfied by this arrangement. Although it is clear that the atomic displacements are influenced by the local vacancy arrangements, the available information on short-range-order parameters is inadequate and it is not possible to proceed further with this topic.

The electronic structure of NbC has recently been calculated (Aoki, Sato, Morinaga, Harada & Adachi, 1988) with the DV-Xα cluster method. Two clusters were examined, (Nb_6C_{12}) and (Nb_6C_{13}), the former with a central vacancy. Here we comment on how these calculations relate to the observed displacements, as this was not reported in the cited publication. The bond order is given in Fig. 9. This value is higher in the presence of a vacancy between C(2*s*, 2*p*) and Nb(4*d*) or between C(2*s*, 2*p*) and Nb(4*d*, 5*s*, 5*p*) than in its absence. This implies that the vacancy enhances the electronic bond strength between Nb and C when these atoms are near a vacancy. Such an interaction would shorten the Nb–C distance, moving Nb away from (and C towards) the vacancy. This is what our analysis indicates. However, the presence of vacancies also enhances Nb–Nb bonding, which would shorten the Nb–Nb interatomic distance. The balance between these two interactions determines the actual displacements and the experimental results

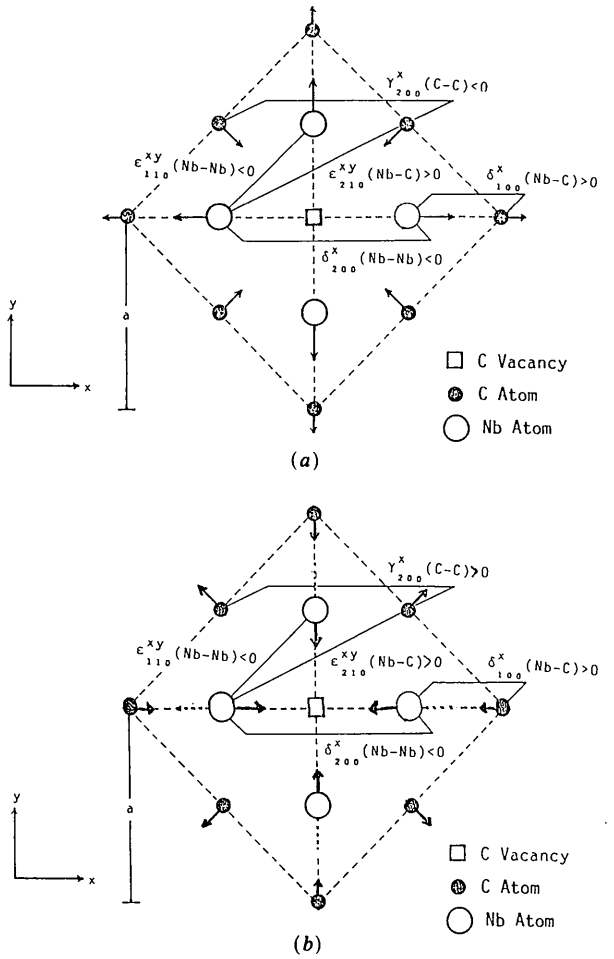

Fig. 6. Models for the atomic displacements. (*a*) Those that satisfy the measured Fourier coefficients. (*b*) The opposite displacements.

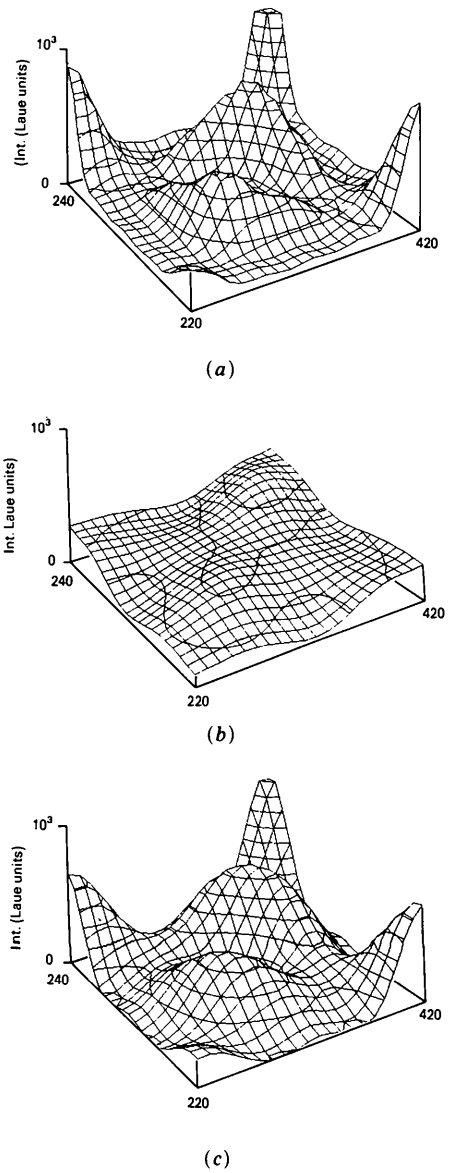

Fig. 7. Comparison of synthesized diffuse intensity maps in the (*hk*0) reciprocal-lattice plane. (*a*) Including all terms. (*b*) Including terms out to (200) vectors. (*c*) Including terms out to (211) vectors. The intensity is in Laue units.

reported here indicate that the first interaction is stronger.

Thus, in summary we note that: (1) the diffuse X-ray (and electron) scattering that has been observed for NbC_x is largely due to static displacements, not local order as had previously been assumed; (2) niobium atoms are displaced away from a carbon-atom vacancy, whereas carbon atoms move towards the vacancy; and (3) there is evidence that the vacancies are arranged in sheets on the {111} planes, not in octahedra as has been suggested in earlier studies.

This joint US-Japan study was supported in the US by a travel grant from the National Science Foundation (grant No. INT-8208308) and by research support from the US Department of Energy (through a subcontract with Purdue University for MATRIX, the Midwest Associated Team for Research with Intense X-rays). For the Japanese investigators, support was provided by the Japan Society for the Promotion of Science. We thank Dr E. Matsubara for his (considerable) advice and assistance during the measurements at CHESS, and are grateful for the cooperation of Professor B. W. Batterman and Dr D. Bildeback of the staff of this storage ring. We also thank Dr S. Sasaki of the Photon Factory, KEK and Professor M. Sakata of Nagoya University for their kind support in programming for the diffuse scattering measurements, and Dr S. Otani of the National Institute for Research on Inorganic Materials for providing the crystal of $NbC_{0.72}$. The Japanese investigators are also grateful to the former directors of the Photon Factory, Professors K. Kohra and T. Sasaki, for promoting this joint project. Finally, we thank Dr C. H. de Novion for pointing out an early error in our calculations.

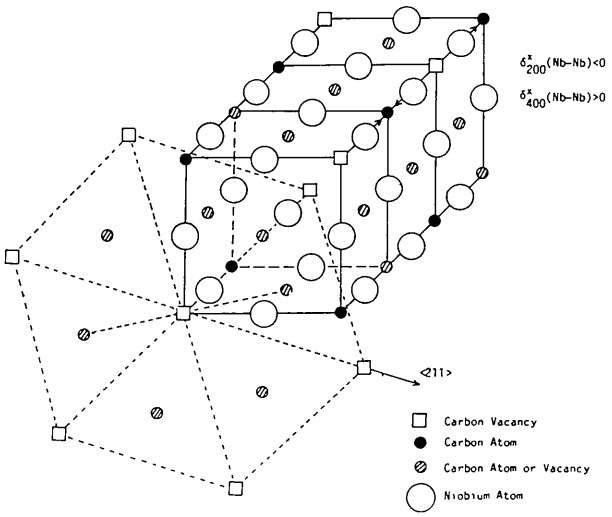

Fig. 8. A possible vacancy arrangement in NbC_x.

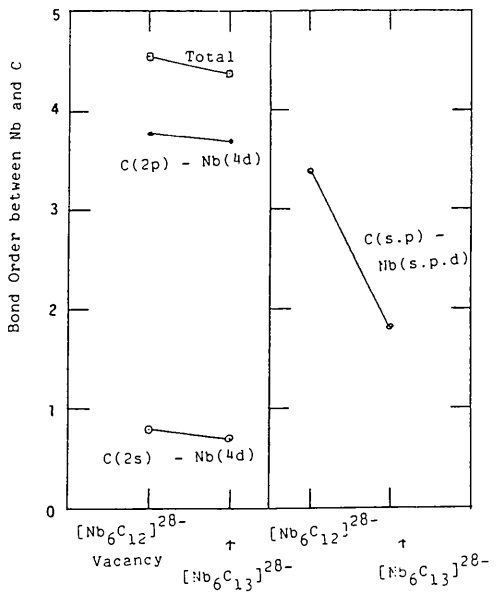

Fig. 9. Change of bond order when vacancies are present.

References

AOKI, A., SATO, K., MORINAGA, M., HARADA, J. & ADACHI, H. (1988). In preparation.

BILLINGHAM, J., BELL, P. S. & LEWIS, M. H. (1972). *Acta Cryst.* A28, 602-606.

BOWMAN, M. G. (1972). *The Chemistry of Fusion Technology*, edited by D. M. GRUEN. Proc. Am. Chem. Soc. Symp. Role of Chemistry in the Development of Controlled Fusion. New York: Plenum Press.

COHEN, J. B. (1986). *Solid State Phys.* **39**, 131-206.

DE RIDDER, R., VAN TENDELOO, G. & AMELINCKX, S. (1975). *Acta Cryst.* A31, S184.

DE RIDDER, R., VAN TENDELOO, G. & AMELINCKX, S. (1976). *Acta Cryst.* A32, 216-224.

GEBALLE, T. H. (1976). In *Critical Materials Problems in Energy Production*, edited by C. STEIN. New York: Academic Press.

GEORGOPOULOS, P. & COHEN, J. B. (1977). *J. Phys. (Paris) Colloq.* C7, 191-196.

GIGRI, A. L., SZKLARZ, E. G., STORMS, E. K., BOWMAN, A. L. & MATTIAS, B. T. (1962). *Phys. Rev.* **125**, 837-838.

HAYAKAWA, M. & COHEN, J. B. (1975). *Acta Cryst.* A31, 635-645.

IIDA, S. (1955). *Progress on Magnetism*, edited by S. CHIKAZUMI, pp. 292-301 (in Japanese). Tokyo: Agne.

KAUFMAN, R. & MEYER, O. (1983). *Phys. Rev. B*, **28**, 6216-6266.

KLEIN, B. M., PAPAKONSTANTOPOULOS, D. A. & BOYER, L. L. (1980). *Phys. Rev. B*, **22**, 1946-1966.

LEWIS, M. H., BILLINGHAM, J. & BELL, P. S. (1972). *Electron Microscopy and Structure of Materials*, edited by E. THOMAS, R. M. FULRATH & R. M. FISHER. Berkeley, CA: Univ. of California Press.

METZGER, H., PEISL, J. & KAUFMAN, R. (1983). *J. Phys. F*, **13**, 1103-1113.

MOISY-MAURICE, V., DE NOVION, C. H., CHRISTENSEN, A. N. & JUST, W. (1981). *Solid State Commun.* **39**, 661-665.

MORINAGA, M. & COHEN, J. B. (1979). *Acta Cryst.* A35, 975-988.

MORINAGA, M., OHSHIMA, K., HARADA, J. & OTANI, S. (1986). *J. Appl. Cryst.* **19**, 417-419.

MORINAGA, M., SATO, K., AOKI, A., ADACHI, H. & HARADA, J. (1983). *Philos. Mag. B*, **47**, 107-111.

OHSHIMA, K., HARADA, J., MORINAGA, M., GEORGOPOULOS, P. & COHEN, J. B. (1986). *J. Appl. Cryst.* **19**, 188-194.

OTANI, S., TANAKA, T. & ISHIZAWA, Y. (1983). *J. Cryst. Growth*, **62**, 211-218.
SAUVAGE, M. & PARTHÉ, E. (1972). *Acta Cryst.* A**28**, 607-616.
SAUVAGE, M. & PARTHÉ, E. (1974). *Acta Cryst.* A**30**, 239-249.
SAUVAGE, M., PARTHÉ, E. & YELON, W. B. (1974). *Acta Cryst.* A**30**, 597-599.
STORMS, E. K. (1967). *The Refractory Carbides.* New York: Academic Press.
TERAUCHI, H. & COHEN, J. B. (1979). *Acta Cryst.* A**35**, 646-652.
TOTH, L. E. (1971). *Transition Metal Carbides and Nitrides.* New York: Academic Press.
TOTH, L. E., ICHIKAWA, M. & CHANG, Y. A. (1968). *Acta Metall.* **16**, 1183-1187.
TOTH, L. E., WANG, C. P. & YEN, C. M. (1966). *Acta Metall.* **14**, 1403-1408.
TOTH, L. E. & ZBASNIK, J. (1968). *Acta Metall.* **16**, 1177-1182.
VENABLES, J. D. & LYE, R. G. (1969). *Philos. Mag.* **19**, 565-582.
WEBER, W. (1973). *Phys. Rev. B*, **8**, 5082-5092.
WILLIAMS, R. O. (1972). Report ORNL 4828. Oak Ridge National Laboratory, TN, USA.
WU, T. B., MATSUBARA, E. & COHEN, J. B. (1983). *J. Appl. Cryst.* **16**, 407-414.

Acta Cryst. (1988). A**44**, 176-183

Direct Methods and Structures Showing Superstructure Effects. III. A General Mathematical Model

BY G. CASCARANO AND C. GIACOVAZZO

Dipartimento Geomineralogico, Università, Campus Universitario, Via Amendola, 70124 *Bari, Italy*

AND M. LUIĆ

Institute 'Rudjer Bošković', Bijenička 54, 41000 *Zagreb, Yugoslavia*

(*Received* 27 *February* 1987; *accepted* 16 *October* 1987)

Abstract

A general mathematical model is presented which can describe a large variety of structures showing superstructure effects. In particular the model can take into account deviations, both of displacive and of replacive type, of the substructural part from ideal pseudotranslational symmetry. The formulation is used to predict statistical effects of deviations on diffraction data. It is shown that the scattering power of the substructural part may be estimated *via* a statistical analysis of diffraction data for ideal pseudotranslational symmetry or for displacive deviation from it, while it is not estimable in the case of replacive deviation.

Symbols and abbreviations

$\mathbf{h}=(h, k, l)$: vectorial index of a reflection.
f: atomic scattering factor. The thermal factor is included; anomalous dispersion is not.
$F_{\mathbf{h}}$: structure factor with vectorial index $\mathbf{h}$.
$\mathbf{C}_s=(\mathbf{R}_s, \mathbf{T}_s)$: sth symmetry operator. $\mathbf{R}_s$ is the rotational part, $\mathbf{T}_s$ the translational part.
N: number of atoms in the cell.
m: order of the space group (it coincides with the number of symmetry operators).
$\mathbf{u}_i$: ith pseudotranslation in the unit cell.
n_i: order of the pseudotranslation $\mathbf{u}_i$.
p: number of atoms (symmetry-equivalent included) whose positions are related by the pseudotranslations $\mathbf{u}$.
q: number of atoms (symmetry-equivalent included) whose positions are not related by any pseudotranslation.
t_p: number of independent atoms which generate the p atoms when the pseudotranslations $\mathbf{u}_i$ and the symmetry operators $\mathbf{C}_s$, $s=1, \ldots, m$ are applied.
t_q: number of independent atoms which generate the q atoms by application of the symmetry operators $\mathbf{C}_s$, $s=1, \ldots, m$.
$\rho(\mathbf{r})$: electron density function in the unit cell.
$\rho_p(\mathbf{r})$, $\rho_q(\mathbf{r})$: electron density functions corresponding to the p atoms and q atoms respectively.
$\varepsilon_{\mathbf{h}}$: weight of the reflexion $\mathbf{h}$ in Wilson's statistics.
$\sum_{t_p}, \sum_{t_q}, \sum_p, \sum_q, \sum_N = \sum f_j^2$ (thermal factor included) where the summation is extended to the t_p, t_q, p, q, N atoms respectively.
$(F_{\mathbf{h}})_p$, $(F_{\mathbf{h}})_q$: structure factors relative to the p and to the q atoms respectively.
$E'_{\mathbf{h}}=F_{\mathbf{h}}/(\varepsilon_{\mathbf{h}}\sum_N)^{1/2}$: normalized structure factor in the absence of any information on pseudotranslational symmetry.
$E_{\mathbf{h}}$: normalized structure factor if prior information on pseudotranslational symmetry is taken into account.
$\varphi_{\mathbf{h}}, \varphi_{\mathbf{k}}, \ldots$: phase of $E_{\mathbf{h}}, E_{\mathbf{k}}, \ldots$.
$[\sigma_r]_p, [\sigma_r]_q, [\sigma_r]_N, \ldots = \sum Z_j^r$, where Z_j is the atomic

0108-7673/88/020176-08$03.00